



HAL
open science

On-Demand Editing of Surface Properties of Microstructures Made by 3D Direct Laser Writing via Photo-Mediated RAFT Polymerization

Xingyu Wu, Bryan Gross, Benjamin Leuschel, Karine Mougín, Sébastien Dominici, Simon Gree, Mehdi Belqat, Vitalii Tkachenko, Benjamin Cabannes-boué, Abraham Chemtob, et al.

► To cite this version:

Xingyu Wu, Bryan Gross, Benjamin Leuschel, Karine Mougín, Sébastien Dominici, et al.. On-Demand Editing of Surface Properties of Microstructures Made by 3D Direct Laser Writing via Photo-Mediated RAFT Polymerization. *Advanced Functional Materials*, In press, 10.1002/adfm.202109446 . hal-03561985

HAL Id: hal-03561985

<https://hal.science/hal-03561985>

Submitted on 8 Feb 2022

HAL is a multi-disciplinary open access archive for the deposit and dissemination of scientific research documents, whether they are published or not. The documents may come from teaching and research institutions in France or abroad, or from public or private research centers.

L'archive ouverte pluridisciplinaire **HAL**, est destinée au dépôt et à la diffusion de documents scientifiques de niveau recherche, publiés ou non, émanant des établissements d'enseignement et de recherche français ou étrangers, des laboratoires publics ou privés.

On-demand Editing of Surface Properties of Microstructures Made By 3D Direct Laser Writing via Photo-mediated RAFT polymerization

Xingyu Wu, Bryan Gross, Benjamin Leuschel, Karine Mougine, Sébastien Dominici, Simon Gree, Mehdi Belqat, Vitalii Tkachenko, Benjamin Cabannes-Boué, Abraham Chemtob, Julien Poly, and Arnaud Spangenberg**

X. Wu, B. Gross, B. Leuschel, K. Mougine, S. Dominici, S. Gree, M. Belqat, V. Tkachenko, B. Cabannes-Boué, A. Chemtob, J. Poly, A. Spangenberg
Institut de Science des Matériaux de Mulhouse (IS2M), CNRS – UMR 7361, Université de Haute Alsace, 15 rue Jean Starcky, 68057 Mulhouse, France
E-mail: xingyu.wu@uha.fr; arnaud.spangenberg@uha.fr

X. Wu, B. Gross, B. Leuschel, K. Mougine, S. Dominici, S. Gree, M. Belqat, V. Tkachenko, B. Cabannes-Boué, A. Chemtob, J. Poly, A. Spangenberg
Université de Strasbourg, France

Keywords: photo-controlled RAFT polymerization, 3D and 4D printing, micro- and nanostructures, surface modification, multi-material printing

Recently, photo-controlled reversible addition-fragmentation chain transfer (RAFT) polymerization has been successfully applied in digital light processing (DLP) 3D printing. It provides a convenient way to tune the surface properties of the 3D printed object. However, so far, 3D micro- and nanostructures and reconfigurations based on photo-induced RAFT polymerization have not been presented. In this work, we apply one macro-photoiniferter, synthesized by photo-controlled RAFT polymerization, to 3D direct laser writing (DLW). Thanks to the exquisite spatial control of the photoreaction, 3D microstructures with feature sizes of around 500 nm are successfully obtained. Taking advantage of the presence of dormant polymeric RAFT agents, photo-induced post-modification of the printed microstructures is highlighted via the elaboration of multi-chemistry patterns including thermo-responsive ones. These results open new perspectives in multi-material and 4D micro-printing.

1. Introduction

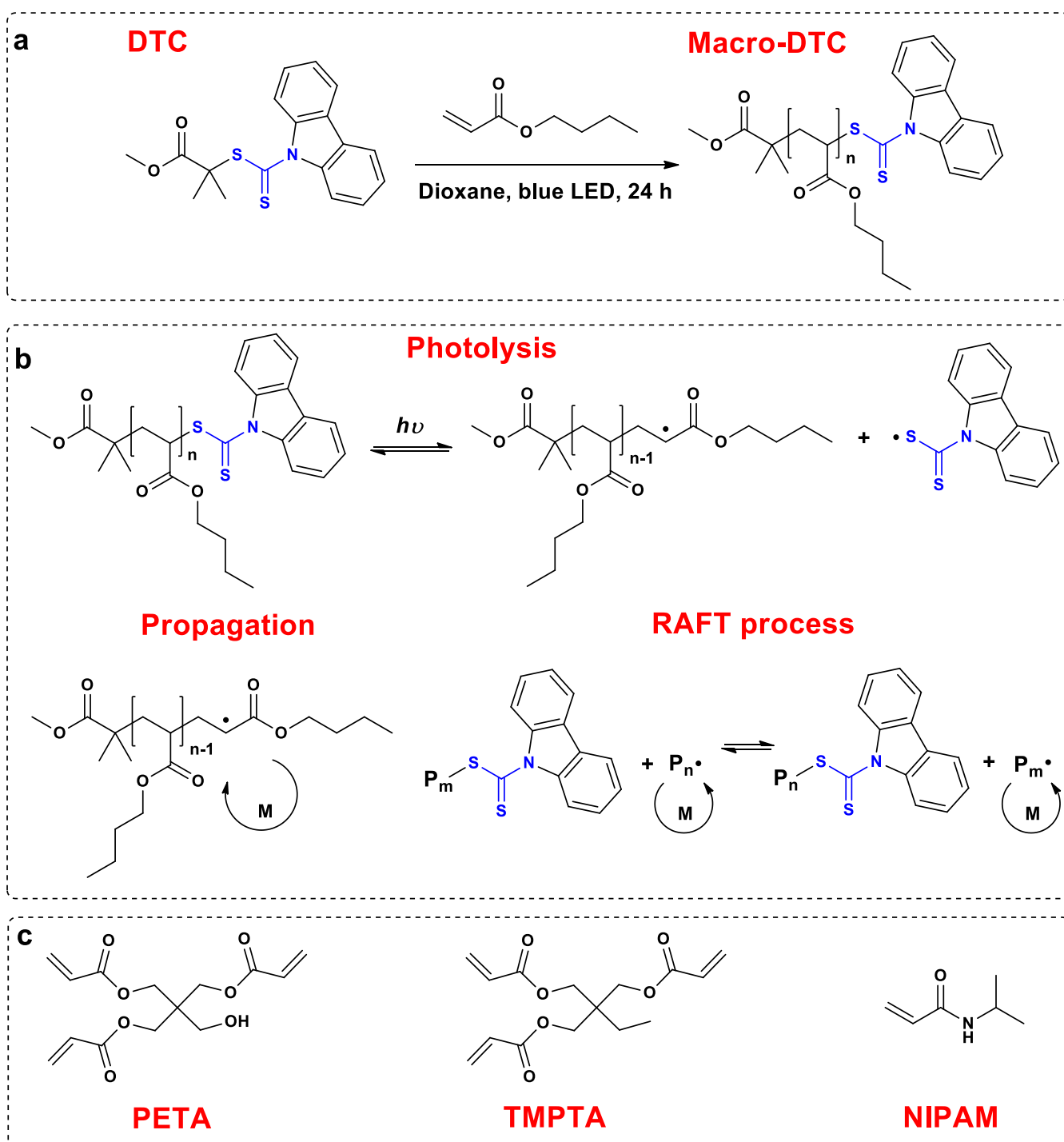
4D printing, originated from Skylar Tibbits, describes the capability of objects to transform over time directly off the print bed.^[1] This fourth dimension requires printed structures to be programmably active and to have the ability to transform independently. This process greatly facilitates the development of multi-material or customized objects for a large number of applications.^[2] However, 3D printing of most current photocurable materials is generally based on conventional radical polymerization. As a result, a polymeric network of “dead” chains is formed due to irreversible termination reactions. Consequently, these chains cannot be used to introduce new monomer units, functionalities or properties in a “living” manner.^[1e,3]

The emergence of photo-controlled living radical polymerization,^[4] especially RAFT polymerization,^[5] opened up new perspectives for 4D printing. In 2017, Johnson et al. developed the first-generation living additive manufacturing process.^[3] In their approach, a 3D “parent” gel was synthesized via click chemistry, and then photo-redox catalyzed RAFT polymerization was carried out to generate “daughter” gels, which could be chemically and mechanically different or similar to “parent” gel. Later, Boyer’s group focused on the direct application of photo-catalyzed RAFT polymerization to the 3D printing process. Their formulations contained an organic dye (photocatalyst), a tertiary amine (co-catalyst), a RAFT agent and acrylates (monomer). A key element for 4D characteristics is the retention of the RAFT chain transfer agent functionality during 3D printing, allowing a facile photochemical post-modification by visible irradiation after the original printing process to tailor surface properties.^[6] Very recently, they proposed to use a Norrish type I photoinitiator instead of photocatalyst in a RAFT polymerization system leading to a faster 3D printing process.^[7]

Surprisingly, to the best of our knowledge, photo-controlled RAFT polymerization has never been described in the context of elaborating 3D micro- and nanostructures by DLW, despite the great potential of this approach for facile surface modifications of such tiny structures. While it is known that micro- and nanostructures with special features have been widely used in photonics,^[8] microelectronics,^[9] biomedicine,^[10] microfluidics^[11] and so on,^[12] a better, more versatile control of surface properties and modifications could lead to new perspectives in these fields.^[13]

In our present work, five macro-photoiniferters (Macro-DTCs, **Scheme 1a** and **Table 1**) were synthesized by photo-controlled RAFT polymerization and one of them (Macro-DTC-01) was selected to perform 3D DLW in presence of air. The initiation system only contains one macro-photoiniferter, no additional compounds. After introducing Macro-DTC-01 into resins, we

investigated its performance in 3D micro-printing. Remarkably, 3D structures with sub-500 nm features could be achieved. Following the fabrication of micro-objects, the dithiocarbamate groups incorporated in the networks were reactivated for reconfiguration processes. Two resins were chosen to customize and modify our microstructures' surfaces: a conventional acrylate resin and a functional, stimuli-responsive material. Detailed experimental procedures can be found in the Supporting Information.



Scheme 1. a) The synthesis process of Macro-DTCs. b) The proposed RAFT polymerization mechanism under irradiation. c) Chemical structures of monomers.

2. Results and Discussion

2.1. Macro-photoiniferters Macro-DTCs

As shown in Scheme 1a, Macro-DTCs are derived from methyl 2-((9*H*-carbazole-9-carbonothioyl)thio)-2-methylpropanoate (DTC). Through RAFT polymerization of butyl acrylate (BA), initiated by DTC, five Macro-DTCs with different number-average molecular weights (M_n) (Table 1) were obtained under blue LED irradiation for 24 hours except in case of Macro-DTC-03. The synthesis processes of DTC and Macro-DTCs are detailed in the Supporting Information and Table 1.^[14] Moreover, Table 1 lists conversion of BA, M_n , and molecular weight dispersity (M_w/M_n) for each of the five Macro-DTCs. The conversions of BA were calculated from ^1H NMR spectra (**Figure S1**), M_n and M_w/M_n were obtained from size exclusion chromatography (SEC, **Figure S2**). The narrow molecular weight distributions, ranging from 1.06 to 1.17 (Table 1), proved that these polymerization processes are well controlled. Based on RAFT polymerization, the mechanism of the polymerization process induced by these macro-photoiniferters is shown in Scheme 1b. Owing to the absorbance of Macro-DTC at blue light (see UV-Vis spectra in **Figure S3**),^[14] photo-excitation of Macro-DTC causes homolytic cleavage of the weak C-S bond, generating a thiocarbonylthio radical and a radical propagating species. The propagating radical species is capable to react with monomer vinyl groups and to interact with other thiocarbonylthio radical species as well as with macromolecules containing dithiocarbamate groups. The recombination of the propagating radical ($P_n\cdot$) with a thiocarbonylthio radical or its reaction with other macro-dithiocarbamates allows a large fraction of the growing polymer chains to become dormant. The retention of the thiocarbonylthio group as a chain-end throughout the polymerization, repeated activations of dormant thiocarbonylthio-capped polymer chains via transfer reactions, and subsequent monomer additions are key elements of RAFT polymerization.^[4g] The ability of a Macro-DTC homologue to initiate polymerization via irradiation at 480 nm or 525 nm has already been investigated in our previous work.^[14] Next, we will explore the capabilities of Macro-DTC in 3D printing.

Table 1. The conversions of BA, M_n and M_w/M_n of Macro-DTCs and their conditions of synthesis under blue LED irradiation.

Macro-DTC	λ_{LED} (nm)	I_{LED} (mW/cm ²)	[BA]/[DTC]	Conversion of BA from ¹ H NMR (%)	M_n of Macro-DTC (kg/mol) ^{a)}	M_w/M_n
Macro-DTC-01	480	96	30	88.9	6.9	1.09
Macro-DTC-02	475	54.6	100	59.4	11.9	1.07
Macro-DTC-03 ^{b)}	475	54.6	100	69.9	14.6	1.06
Macro DTC-04	480	96	100	91.0	18.8	1.14
Macro-DTC-05	480	96	150	94.7	26.7	1.17

^{a)} determined by SEC in THF eluent. ^{b)} the reaction time is 29 hours, instead of 24 hours.

2.2. 3D printing

3D DLW is a very useful tool to generate arbitrary microstructures. In this work, all 2D and 3D printing were performed on a high resolution 3D-printing system (μ FAB-3D from Microlight3D) based on DLW at 532 nm. The fabrication procedure is illustrated in **Figure 1a** and the printing parameters are detailed in the Supporting Information.

First, we have investigated the performance of Macro-DTC-01/PETA in the printing of 2D microstructures. Pentaerythritol triacrylate (PETA, chemical structure is shown in Scheme 1c) is a trifunctional monomer, which was added to the formulation as crosslinker to improve the mechanical stability of the resulting microstructures. In order to preserve the ability of the polymer to undergo repolymerization, we first used a limited amount of PETA (20 wt%). However, as highlighted in **Figure S4** (right), the degree of crosslinking within the polymer microstructure was not sufficient to maintain structural integrity after development. By increasing the amount of PETA up to 50 wt%, mechanically stable 3D microstructures were successfully fabricated (Figure S4, left). Therefore, formulations based on Macro-DTC/PETA (50/50, wt%) were systematically employed in all of the following experiments. Furthermore, we studied the impact of the M_n on fabrication conditions, features' size and structuration. For each formulation listed in **Table 2**, we have first determined the intensity threshold I_{th} and the damage intensity I_{damage} defined respectively as the minimum laser intensity required to initiate the polymerization and the laser intensity leading to micro-explosion. To that aim, lines were fabricated at increasing laser intensity with a printing speed of 14.3 μ m/s. The results are

reported for each formulation in Table 2 and a representative series of lines is given for the formulation Macro-DTC-01/PETA (**Figure S5**). One can notice that the intensity threshold I_{th} is higher for higher number average molecular weight M_n , underlining a lower reactivity for formulation based on Macro-DTC with high M_n . This can be explained by a lower concentration of DTC groups for high M_n Macro-DTC. No obvious changes in the damage intensity I_{damage} were observed. In a second step, we have investigated the impact of laser intensity on the feature size of microstructures. Thus, single-voxel structures were prepared from formulations based on Macro-DTC/PETA (50/50, wt%, Table 2) at different laser intensities, while keeping a constant exposure time (10 ms). Then, their heights were measured subsequently from SEM images. Similar experiments were conducted with PETA/Macro-DTC-01 to 05, and the voxel heights were plotted as a function of laser intensities (**Figure S6**). As expected, higher intensity leads to increased voxel dimensions and consequently to lower resolution. Interestingly, Macro-DTC-01/PETA exhibits the broader window processability by allowing creation of voxel from 0.25 mW/cm² to 2.3 mW/cm², leading to heights from 2.5 to 9 μ m. To confirm the better printability provided by Macro-DTC-01/PETA, woodpile microstructures were made from all formulations from Table 2 with a laser intensity close to the laser intensity threshold I_{th} of each formulation and a printing speed of 14.3 μ m/s. The formulation Macro-DTC-01/PETA clearly leads to the best performance in terms of structuration (**Figure S7**). Moreover, as shown by Luo and coworkers,^[15] increasing the number of DTC groups in the starting formulation will favor the number of DTC groups in the final polymer. Therefore in order to optimize structuration capability and the ability of the microstructure to be post-functionalized, the formulation Macro-DTC-01/PETA has been selected for the next sections.

Table 2. Compositions and reactivities of formulations based on Macro-DTC/PETA.

Macro-DTC/PETA (50/50 wt%)	Macro-DTC (g)	n of Macro-DTC (μ mol)	I_{th} (mW/cm ²)	I_{damage} (mW/cm ²)
Macro-DTC-01/PETA	0.262	38.0	0.248	2.3
Macro-DTC-02/PETA	0.252	21.2	0.446	2.3
Macro-DTC-03/PETA	0.245	16.8	0.550	2.3
Macro DTC-04/PETA	0.246	13.1	0.99	2.3
Macro-DTC-05/PETA	0.283	10.6	1.58	2.3

To demonstrate Macro-DTC-01's performance in DLW, two intricate 3D structures were achieved with a laser intensity of 0.38 mW/cm^2 and a printing speed of $43.4 \text{ }\mu\text{m/s}$. SEM images (Figure 1b) show that the structures have well defined shapes and sub- μm resolutions ($\sim 500 \text{ nm}$). Here, it is worth noting that these structures were made from a formulation which contained 50 wt% PETA and 50 wt% Macro-DTC, no other additives. These complex microstructures prove Macro-DTC-01 is an excellent photoiniferter for photopolymerization processes during 3D printing.

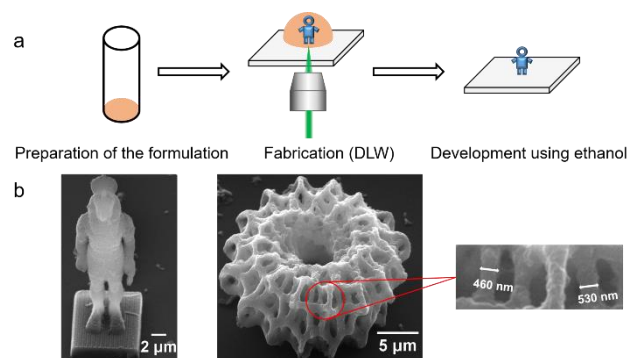


Figure 1. a) The process to fabricate 3D micro-objects using DLW. b) SEM images of 3D microstructures made from PETA and Macro-DTC-01 (50:50, wt%) using a printing speed of $43.4 \text{ }\mu\text{m/s}$ and a laser intensity of 0.38 mW/cm^2 . The red circle is used to point to the zoom-in image to see the resolution.

2.3. Multi-material microstructures

Several experiments were conducted in order to study the possibility to perform localized modifications of 3D microstructures, thanks to the presence of dithiocarbamate groups in the formed polymer. As shown in **Figure 2a** (top), we used pure trimethylolpropane triacrylate (TMPTA, chemical structure is shown in Scheme 1c) without Macro-DTC to write the letters “ μRAFT ” onto an assembly of microstructures, created via successive functionalizations of a variable number of layers on top of a PETA base microstructure. Figure 2b shows the “ μRAFT ” fabricated onto the top of three different, stacked squares. Amongst those squares, exclusively the bottom-layer square ($50 \times 50 \text{ }\mu\text{m}^2$) was made from 50 wt% PETA and 50 wt% Macro-DTC-01 using a laser intensity of 0.44 mW/cm^2 and a printing speed of $14.3 \text{ }\mu\text{m/s}$, every subsequent square (repolymersed layer) was made from pure TMPTA without Macro-DTC. The intensities used for fabricating the second and third squares were 0.85 and 0.99 mW/cm^2 , while the printing speed was kept at $14.3 \text{ }\mu\text{m/s}$ and resulted in layer thicknesses of 240 and 277 nm , respectively (**Figure S8**). As shown in the AFM and SEM images (Figure 2b, **Figure S9**), the

height of letters on the top layer (1.92 mW/cm^2) is 217 nm and their width 200 nm. Here, the uniform height and exceptionally high resolution of the microstructures on the final layer clearly proves the successful repolymerization. Moreover, reinitiation, reconfigurations and modifications can be achieved, remarkably, across multiple layers using Macro-DTC-01. One major advantage of living polymerization is that it guarantees covalent linking of the microstructures to the supporting polymer surface, which greatly eliminates the adhesion problems between layers. In order to confirm the presence of DTC groups into the repolymerized layers (with a total thickness of $1.4 \text{ }\mu\text{m}$, **Figure S10**), micro-FTIR experiments were conducted. In **Figure S11**, we can clearly see peaks at 1666 cm^{-1} (aromatic C–H), 1451 cm^{-1} (aromatic C=C), 1326 cm^{-1} (C=S) and 755 cm^{-1} (aromatic C–H and C–S) in the spectrum of the repolymerized layers, which are characteristic peaks of dithiocarbamate.^[16] The experimental details are described in the Supporting Information. Finally, it has to be mentioned that no polymerization or repolymerization was observed in pure TPMTA or in absence of Macro-DTC in the conditions of excitation for fabrication and functionalization (**Figure S12** and **S13**). These control experiments confirm the crucial role played by Macro-DTC in allowing fabrication and functionalization of microstructures. Based on these observations, one can assume that the multi-layer growth process is induced by photo-mediated RAFT polymerization.

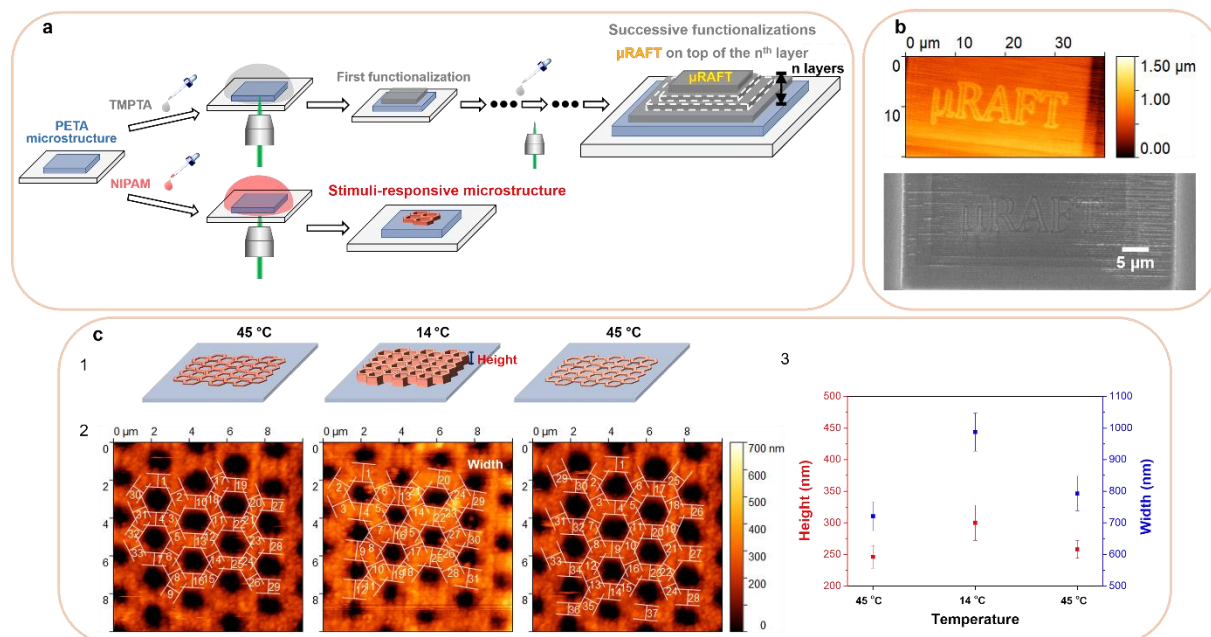


Figure 2. a) The process to modify the surface of microstructures using DLW. b) AFM and SEM images of μRAFT at the top layer made from TMPTA without photoinitiator. The first layer is a square made from PETA and Macro-DTC-01 (50:50, wt%), other squares (repolymerized layers) are made from TMPTA alone. c) The evolution of PNIPAM honeycomb microstructures on the square at different temperatures. 1) The schema to illustrate the change

of heights. 2) AFM images with profile indicators (white lines). 3) The heights and widths measured from AFM images. For all fabrications and post-functionalizations, the printing speed was set to 14.3 $\mu\text{m/s}$.

To further demonstrate the versatility of this RAFT polymerization, a spatially controlled polymerization process using *N*-isopropylacrylamide (NIPAM, Scheme 1c) monomers was performed on the surface of polymerized Macro-DTC-01/PETA squares. Poly (*N*-isopropylacrylamide) (PNIPAM) is well-known as a temperature-responsive polymer hydrogel, which has been used in the fields of biosensors, actuators and drug delivery.^[17] Raising the temperature above the lower critical solution temperature (LCST) of PNIPAM causes it to become hydrophobic and dehydrate, i.e. PNIPAM expels water molecules from the spaces in its polymer network, which results in shrinkage and stiffening of the structure. Upon decreasing the temperature, this process reverses and PNIPAM returns to its swollen, hydrated state. Even though several attractive 3D-printed PNIPAM structures were presented, it remains a challenge to obtain PNIPAM structures exhibiting this temperature stimulus response.^[18] This is due to the ratio of monomer to crosslinker used for fabrication: with low quantities of crosslinker, it can hardly form structures, even if the resulting material responds to the stimulus; on the other hand, with high amounts of crosslinker, it can easily produce arbitrary structures, which, however, hardly respond to temperature. In our experiment, Macro-DTC-01 allows us to fabricate responsive patterns via reconfigurations of the surface of a base microstructure. The formulation used for post-modification contains only NIPAM and ethylene glycol. First, as before, a square was made using 50 wt% PETA and 50 wt% Macro-DTC-01; then a drop of the NIPAM solution was applied to cover the square (Figure 2a bottom). A well-organized honeycomb structure was patterned onto the square (Figure 2c) using DLW (1.50 mW/cm²) followed by development using ethanol. The stimuli-responsive property of PNIPAM has been investigated using AFM in an aqueous environment. When the water temperature is 45 °C, the heights are 246 nm (± 18 nm), measured from the top of the PETA square to the top of the bars and the widths are 721 nm (± 46 nm). After decreasing the temperature to 14 °C, both heights (300 ± 14 nm) and widths (987 ± 60 nm) increase, compared to their dimensions at 45 °C. When the water is heated again to 45 °C, the sizes of structures decrease again as well (heights 258 ± 14 nm, widths 793 ± 55 nm). Figure 2c1 illustrates the evolution of PNIPAM microstructures in height. The AFM images (Figure 2c2) let us easily perceive the changes in height via differing color-map values, and changes in width through variations of the sizes of holes. To quantify these changes, the heights and widths at each temperature are plotted in

Figure 2c3. Clearly, Figure 2c shows PNIPAM's shrunk and swollen states under water. Here, it is worth to mention that upon cooling from 45 °C to 14 °C, the structures' heights increase less than their widths. This may be attributed to the organization of polymer chains, which deserves to be further studied.

To highlight the potential of our approach, the functionalization of a 3D microstructure were carried out. For this purpose, one “bridge” microstructure, consisting of four pillars connected by four horizontal hanging bars, was fabricated (0.38 mW/cm², 43.4 μm/s) from Macro-DTC-01/PETA (50/50, wt%) (**Figure 3a**). Then, functionalization was performed on one of the hanging bars using TMPTA with fluorescein (1.78 mW/cm², 14.3 μm/s) (Figure 3b). Fluorescein has been added to the TMPTA to allow visualization of the functionalized part via fluorescence lifetime imaging (FLIM). It has to be noted that similar structures were also obtained without fluorescein. As shown in the inset of the SEM image after functionalization (Figure 3a), the repolymerized structure is localized on the top of one hanging bar, demonstrating the exquisite control in the spatial modification of the polymerized microstructure. The height of the functionalized area was estimated to 720 nm from the inset SEM image.

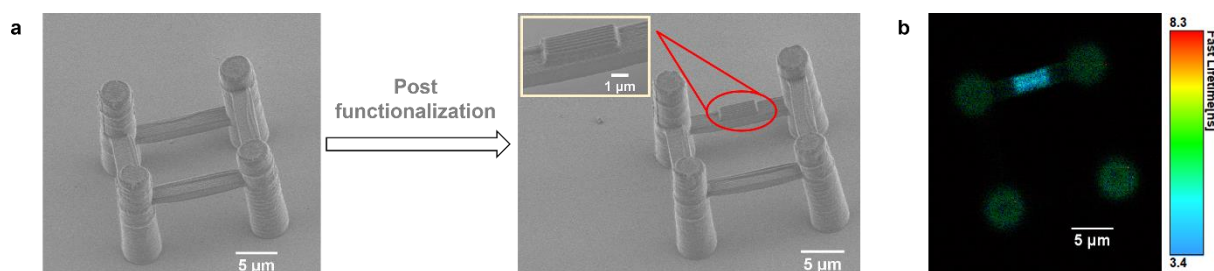


Figure 3. a) SEM images (tilt view) of bridges made from Macro-DTC-01/PETA (50:50, wt%) without (left) and with (right) functionalization from TMPTA with fluorescein. Inset: zoom on the functionalized area. b) FLIM image (top view) of the functionalized bridge.

2.4. Intensity-mediated surface modification

To further explore the conditions for optimal surface modification, several groups of lines (**Figure 4a**) made from pure TMPTA without Macro-DTC were fabricated on the assembled squares. The laser intensities used for the first to fourth square were 0.44, 0.85, 0.99 and 1.15 mW/cm², respectively. The first square corresponds to the first polymerized layer, while the second and further squares correspond to repolymerized layers. The distance between two adjacent lines is 3 μm. The laser intensity was increased gradually between lines, while keeping printing speed constant at 14.3 μm/s. In Figure 4b, lines' heights, measured by AFM (Figure

4c), are plotted against laser intensity. The heights increase linearly with laser intensity, except for the lines on the first layer at intensities above 2.1 mW/cm². From Figure 4b, one can also notice that the heights of repolymerized lines clearly decrease with an increasing number of consecutive layers. For instance, while for the lines on the top of the first layer the height is ranging from 100 nm to 1000 nm in function of laser intensity, for the lines on the top of the fourth layer, the height is only tunable between 15 to 220 nm for the same range of laser intensities. Similar trends are observed for lines' widths against laser layer intensity (**Figure S14**). These observations can probably be explained by the formation of dead polymer chains during the whole process. While this indicates that the number of possible successive repolymerizations is certainly limited, this set of data nicely demonstrates that several consecutive post-functionalizations or modifications can be realized in a controlled manner by varying laser intensity. Indeed, the heights of these structures can be tuned accurately from nano- up to micro-scale which is very important in surface functionalization and surface patterning applications.^[19]

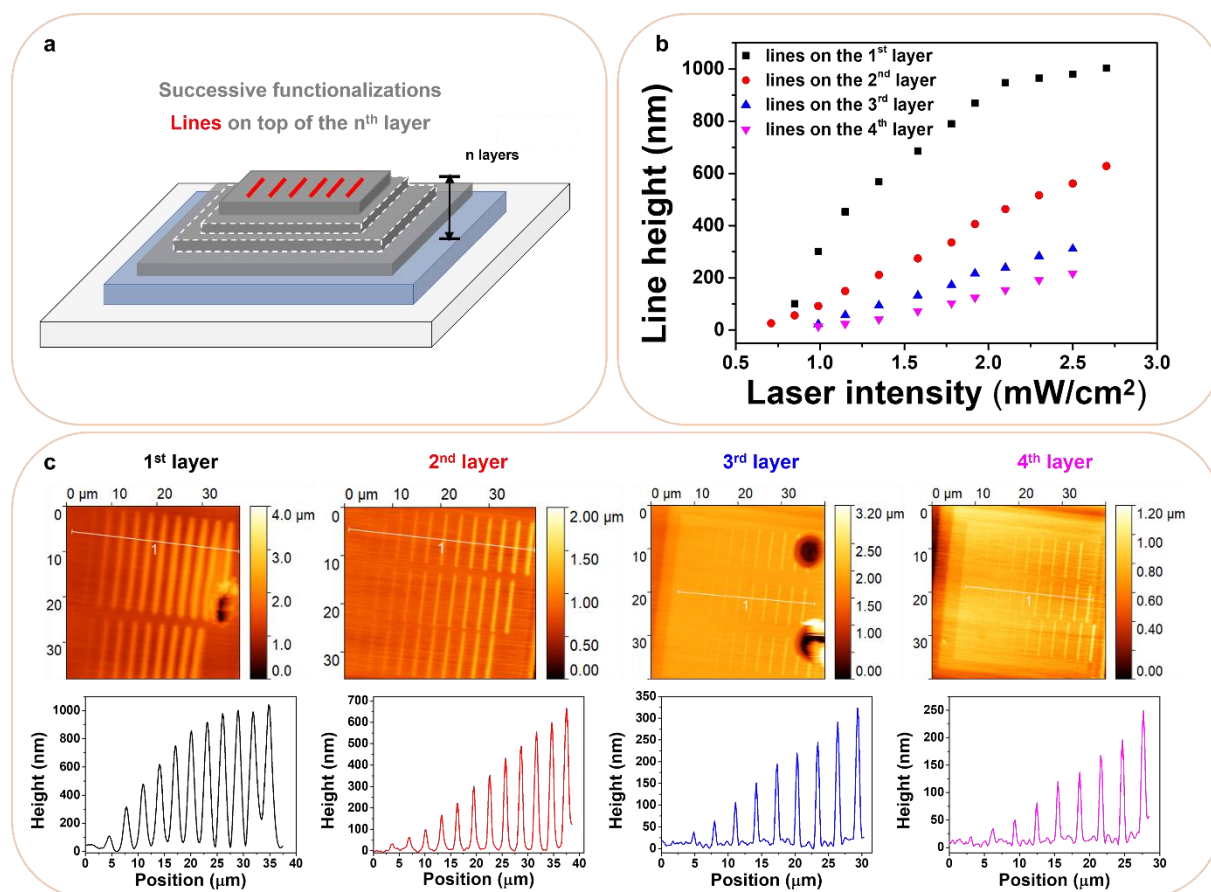


Figure 4. a) Layout of assembled square layers with lines. b) The height of lines at the first to fourth layer made from TMPTA alone as a function of laser intensity. The first layer is a square made from PETA and Macro-DTC-01 (50:50, wt%). c) AFM images of these lines and profiles. For all fabrications, the printing speed was fixed to 14.3 $\mu\text{m/s}$.

3. Conclusion

In summary, we have applied a macro-photoiniferter synthesized by photo-controlled RAFT polymerization for the creation and reconfiguration of 3D microstructures by DLW in presence of air. The simple formula system (Macro-DTC plus one resin) makes sample preparation easy and greatly reduces migration problems during fabrication and in structures. Remarkably, this Macro-DTC is suitable for the fabrication of arbitrary 3D structures with sub-500 nm resolution by DLW, while its retention of RAFT functionalities throughout successive functionalization steps allows the versatile reconfiguration of surfaces across multiple layers and using different materials, e.g. temperature-sensitive polymers. By adapting light intensity and materials, well-defined structures with controlled dimensions and tailored properties can be patterned. The combination of this photo-controlled RAFT polymerization process with 3D DLW provides a strategy to fabricate and reconfigure 3D microstructures by affording access to new functional and stimuli-responsive materials for 4D and multi-material micro-printing.

Supporting Information

Supporting Information is available from the Wiley Online Library or from the author.

Acknowledgements

The authors thank the Agence Nationale de la recherche (Project ANR 2PhotonInsight: ANR-16-CE08-347 0020) and Institut Carnot MICA for financial support. B.G, Dr. J.P. and Dr. A.S. thank the IS2M for an emergent grant. This work was also partially supported by an Institutional Research Grant (MIPPI4D) from the Région Grand Est. The authors thank Tatiana Petithory and Ludovic Josien for their help in fluorescence microscopy and SEM, respectively.

The authors declare no competing financial interests.

Received: ((will be filled in by the editorial staff))

Revised: ((will be filled in by the editorial staff))

Published online: ((will be filled in by the editorial staff))

References

- [1] a) S. Tibbits, *Architectural Design* **2014**, *84*, 116; b) J. Lee, H.-C. Kim, J.-W. Choi, I. H. Lee, *Int. J. of Precis. Eng. and Manuf.-Green Tech.* **2017**, *4*, 373; c) F. Momeni, X. Liu, J.

Ni, *Mater. Des.* **2017**, *122*, 42; d) I. Roppolo, A. Chiappone, A. Angelini, S. Stassi, F. Frascella, C. Pirri, C. Ricciardi, E. Descrovi, *Mater. Horiz.* **2017**, *4*, 396; e) A. Bagheri, J. Jin, *ACS Appl. Polym. Mater.* **2019**, *1*, 593; f) X. Kuang, D. J. Roach, J. Wu, C. M. Hamel, Z. Ding, T. Wang, M. L. Dunn, H. J. Qi, *Adv. Funct. Mater.* **2019**, *29*, 1805290.

[2] a) B. Gao, Q. Yang, X. Zhao, G. Jin, Y. Ma, F. Xu, *Trends Biotechnol.* **2016**, *34*, 746; b) Q. Ge, A. H. Sakhaei, H. Lee, C. K. Dunn, N. X. Fang, M. L. Dunn, *Sci. Rep.* **2016**, *6*, 31110; c) A. S. Gladman, E. A. Matsumoto, R. G. Nuzzo, L. Mahadevan, J. A. Lewis, *Nat. Mater.* **2016**, *15*, 413; d) M. Zarek, M. Layani, I. Cooperstein, E. Sachyani, D. Cohn, S. Magdassi, *Adv. Mater.* **2016**, *28*, 4449; e) S. Dutta, D. Cohn, *J. Mater. Chem. B* **2017**, *5*, 9514; f) H. Yang, W. R. Leow, T. Wang, J. Wang, J. Yu, K. He, D. Qi, C. Wan, X. Chen, *Adv. Mater.* **2017**, *29*, 1701627; g) A. Kotikian, R. L. Truby, J. W. Boley, T. J. White, J. A. Lewis, *Adv. Mater.* **2018**, *30*, 1706164; h) Z. Zhao, X. Kuang, C. Yuan, H. J. Qi, D. Fang, *ACS Appl. Mater. Interfaces* **2018**, *10*, 19932; i) K. Jung, N. Corrigan, M. Ciftci, J. Xu, S. E. Seo, C. J. Hawker, C. Boyer, *Adv. Mater.* **2020**, *32*, 1903850.

[3] M. Chen, Y. Gu, A. Singh, M. Zhong, A. M. Jordan, S. Biswas, L. T. J. Korley, A. C. Balazs, J. A. Johnson, *ACS Cent. Sci.* **2017**, *3*, 124.

[4] a) Y. Kwak, K. Matyjaszewski, *Macromolecules* **2010**, *43*, 5180; b) B. P. Fors, C. J. Hawker, *Angew. Chem., Int. Ed.* **2012**, *51*, 8850; c) B. P. Fors, J. E. Poelma, M. S. Menyo, M. J. Robb, D. M. Spokoyny, J. W. Kramer, J. H. Waite, C. J. Hawker, *J. Am. Chem. Soc.* **2013**, *135*, 14106; d) F. A. Leibfarth, K. M. Mattson, B. P. Fors, H. A. Collins, C. J. Hawker, *Angew. Chem., Int. Ed.* **2013**, *52*, 199; e) K. Matyjaszewski, N. V. Tsarevsky, *J. Am. Chem. Soc.* **2014**, *136*, 6513; f) S. Telitel, F. Dumur, S. Telitel, O. Soppera, M. Lepeltier, Y. Guillaneuf, J. Poly, F. Morlet-Savary, P. Fioux, J.-P. Fouassier, *Polym. Chem.* **2015**, *6*, 613; g) M. Chen, M. Zhong, J. A. Johnson, *Chem. Rev.* **2016**, *116*, 10167; h) C. Kütahya, C. Schmitz, V. Strehmel, Y. Yagci, B. Strehmel, *Angew. Chem., Int. Ed.* **2018**, *57*, 7898; i) J. Yeow, R. Chapman, A. J. Gormley, C. Boyer, *Chem. Soc. Rev.* **2018**, *47*, 4357.

[5] a) Y. Amamoto, J. Kamada, H. Otsuka, A. Takahara, K. Matyjaszewski, *Angew. Chem., Int. Ed.* **2011**, *50*, 1660; b) H. Zhou, J. A. Johnson, *Angew. Chem., Int. Ed.* **2013**, *52*, 2235; c) M. B. Gordon, J. M. French, N. J. Wagner, C. J. Kloxin, *Adv. Mater.* **2015**, *27*, 8007; d) G. Ng, J. Yeow, J. Xu, C. Boyer, *Polym. Chem.* **2017**, *8*, 2841; e) E. E. Stache, V. Kottisch, B. P. Fors, *J. Am. Chem. Soc.* **2020**, *142*, 4581.

[6] a) Z. Zhang, N. Corrigan, A. Bagheri, J. Jin, C. Boyer, *Angew. Chem., Int. Ed.* **2019**, *58*, 17954; b) A. Bagheri, C. W. A. Bainbridge, K. E. Engel, G. G. Qiao, J. Xu, C. Boyer, J. Jin, *ACS Appl. Polym. Mater.* **2020**, *2*, 782; c) X. Shi, J. Zhang, N. Corrigan, C. Boyer, *Mater.*

- Chem. Front.* **2021**, *5*, 2271; d) Z. Zhang, N. Corrigan, C. Boyer, *Macromolecules* **2021**, *54*, 1170.
- [7] K. Lee, N. Corrigan, C. Boyer, *Angew. Chem., Int. Ed.* **2021**, *60*, 8839.
- [8] a) A. Ovsianikov, J. Viertl, B. Chichkov, M. Oubaha, B. MacCraith, I. Sakellari, A. Giakoumaki, D. Gray, M. Vamvakaki, M. Farsari, C. Fotakis, *ACS Nano* **2008**, *2*, 2257; b) A. Vyatskikh, R. C. Ng, B. Edwards, R. M. Briggs, J. R. Greer, *Nano Lett.* **2020**, *20*, 3513.
- [9] S. Y. Yu, G. Schrodj, K. Mouglin, J. Dentzer, J. P. Malval, H. W. Zan, O. Soppera, A. Spangenberg, *Adv. Mater.* **2018**, *30*, 1805093.
- [10] U. Bozuyuk, O. Yasa, I. C. Yasa, H. Ceylan, S. Kizilel, M. Sitti, *ACS Nano* **2018**, *12*, 9617.
- [11] a) K. Sugioka, J. Xu, D. Wu, Y. Hanada, Z. Wang, Y. Cheng, K. Midorikawa, *Lab Chip* **2014**, *14*, 3447; b) H. Wang, Y.-L. Zhang, W. Wang, H. Ding, H.-B. Sun, *Laser Photonics Rev.* **2017**, *11*, 1600116.
- [12] a) H. Xia, J. Wang, Y. Tian, Q.-D. Chen, X.-B. Du, Y.-L. Zhang, Y. He, H.-B. Sun, *Adv. Mater.* **2010**, *22*, 3204; b) F. Klein, B. Richter, T. Striebel, C. M. Franz, G. v. Freymann, M. Wegener, M. Bastmeyer, *Adv. Mater.* **2011**, *23*, 1341; c) Y.-L. Sun, W.-F. Dong, R.-Z. Yang, X. Meng, L. Zhang, Q.-D. Chen, H.-B. Sun, *Angew. Chem., Int. Ed.* **2012**, *51*, 1558; d) T. Bückmann, N. Stenger, M. Kadic, J. Kaschke, A. Frölich, T. Kennerknecht, C. Eberl, M. Thiel, M. Wegener, *Adv. Mater.* **2012**, *24*, 2710; e) H. Zeng, D. Martella, P. Wasylczyk, G. Cerretti, J.-C. G. Lavocat, C.-H. Ho, C. Parmeggiani, D. S. Wiersma, *Adv. Mater.* **2014**, *26*, 2319; f) Y. Lin, J. Xu, *Adv. Opt. Mater.* **2018**, *6*, 1701359; g) H. Ding, Q. Zhang, H. Gu, X. Liu, L. Sun, M. Gu, Z. Gu, *Adv. Funct. Mater.* **2020**, *30*, 1901760; h) D. Jin, Q. Chen, T.-Y. Huang, J. Huang, L. Zhang, H. Duan, *Mater. Today* **2020**, *32*, 19.
- [13] a) H. Ceylan, I. C. Yasa, M. Sitti, *Adv. Mater.* **2017**, *29*, 1605072; b) D. W. Yee, M. D. Schulz, R. H. Grubbs, J. R. Greer, *Adv. Mater.* **2017**, *29*, 1605293.
- [14] B. Cabannes-Boué, Q. Yang, J. Lalevée, F. Morlet-Savary, J. Poly, *Polym. Chem.* **2017**, *8*, 1760.
- [15] N. Luo, A. T. Metters, J. B. Hutchison, C. N. Bowman, K. S. Anseth, *Macromolecules* **2003**, *36*, 6739.
- [16] a) R. Guo, X. Wang, C. Guo, A. Dong, J. Zhang, *Macromol. Chem. Phys.* **2012**, *213*, 1851; b) M. Ates, N. Uludag, F. Arican, *Polym. Bull.* **2014**, *71*, 1557.
- [17] L. Tang, L. Wang, X. Yang, Y. Feng, Y. Li, W. Feng, *Prog. Mater. Sci.* **2021**, *115*, 100702.

- [18] a) M. Hippler, E. Blasco, J. Qu, M. Tanaka, C. Barner-Kowollik, M. Wegener, M. Bastmeyer, *Nat. Commun.* **2019**, *10*, 232; b) A. Nishiguchi, H. Zhang, S. Schweizerhof, M. F. Schulte, A. Mourran, M. Möller, *ACS Appl. Mater. Interfaces* **2020**, *12*, 12176.
- [19] Z. Nie, E. Kumacheva, *Nat. Mater.* **2008**, *7*, 277.